Hittite Journal of Science and Engineering, 2018, 5 (2) 155-164
ISSN NUMBER: 2148-4171
DOI: 10.17350/HJSE19030000090

Thermal Behaviour of Residential Buildings with Cantilever Beams under Winter Boundary Conditions

Lütfü Namli
Ondokuz Mayis University, Department of Mechanical Engineering, Samsun, Turkey

ABSTRACT

In this study, the thermal behaviour of residential buildings with cantilever beam under winter boundary conditions was numerically investigated by means of the open-ended structure approach. For this purpose, parametric studies were carried out for various ratios of cantilever beam depth/cantilever beam height (d/H) and Rayleigh numbers using a computer program for no wind laminar flow conditions. Analyses were conducted for Rayleigh numbers in the range of 10^3 to 10^6. The calculations were carried out for the ratios of d/H, namely 0.0, 0.2, 0.4, 0.6, 0.8 and 1.0. The working fluid was treated as air (Pr=0.71). According to the findings, the mean Nu number along with the outer vertical wall (surface L) of the residential building, in general, decreases as d/H increases. This decrease in the mean Nu number is evident for $Ra \leq 10^4$, but it appears to be more pronounced after $Ra=10^5$. To have minimum heat loss from a residential building under winter day boundary conditions, it is suggested that the ratio of d/H should be between 0.2 and 0.5.

Article History:
Received: 2017/07/16
Accepted: 2017/12/20
Online: 2017/12/26

***Correspondence to**: Lütfü Namlı, Department of Mechanical Engineering, Ondokuz Mayis University, Samsun, Turkey*
e-mail: lnamli@omu.edu.tr

Keywords:
Open-ended structure; Extended boundaries; Cantilever beam; Laminar natural convection

INTRODUCTION

In recent years, the fluid flow and heat transfer phnomena surrounding open-ended cavities or enclosures related to the natural convection mechanism have received significant interest from many researchers, both numerically and experimentally. There are many reasons for this interest. In particular, several applications of practical interest, such as thermal building insulation by means of air gaps, solar energy collectors, fire control in buildings, thermal storage systems, and electronic cooling in which can be modelled by different extensions of similar geometry [1-2]. One such field of application is a thermal performance in residential buildings. Residential buildings are one of the most important energy consumers in the world. Approximately 30% of European and Middle Eastern energy consumption occurs in residential buildings [3-5]. Reducing thermal energy consumption is, therefore, an important issue facing the building industry. However, the great majority of studies on the thermal performance of residential buildings have focused on insulating them by applying various building envelopes [5-7]. However, an equally important matter is the exterior geometry of the buildings. The literature related to the effects of building exterior geometry on the thermal performance of residential buildings has not been adequately studied. Current studies are usually concerned with examining the effects of exterior geometry on the interior ventilation of a building [8]. One of the most important structures that form the external geometry of residential buildings is the cantilever beam, which is very common in many countries, e.g. Turkey [7]. In this field, numerous efforts have been taken to analyse these rectangular cavities, which are often two-dimensional. Two-dimensional natural convection related to cavities or enclosures comprises a large proportion of these analyses in the literature. However, a relevant but more complicated problem related to open-ended or partial enclosures cavities has attracted less attention. The two-dimensional natural convection related to open-ended enclosures (cavities) have been examined by many researchers in the cited literature in the past four decades [9, 10]. Chan and Tien [10] carried out a numerical laminar natural convection study for a two-dimensional open-ended enclosure having a vertical wall. In this study, the vertical wall of the enclosure was heated and the other two horizontal walls of the enclosure were insulated. The study results indicated the influences of the extended boundary on the main flow

forms. Analyses were performed in the computational zone extended along with the open plane of the open-ended cavity for Rayleigh numbers ranging from 103 to 109. The same authors [10] also calculated the steady-state laminar natural convection in a two-dimensional rectangular open-ended cavity by applying the proximate boundary circumstances at the enclosure open plane. A detailed study was carried out by Vafai and Ettfagh [11, 12] to analyse the characteristics and physics of flow areas in enclosures. The same authors [11, 12] also studied the extended computational zone effect upon fluid flow and heat transfer in an enclosure and its immediate environment. Similarly, many researchers have studied buoyancy-driven fluid flow and heat transfer within enclosures that have one side open by giving particular importance to their outer approximate confines. The studies cited in the literature have concentrated on obtaining an exact representation of the prevalent boundary circumstances at the open plane in both two- and three-dimensional open-ended cavities [13-16].

The effects of cantilever beam applications, which are commonly encountered in buildings and other constructions in many countries, on the thermal behaviour of residential buildings are subjects which can be analysed in the scope of the natural convection subject using an open-cavity approach. In the literature, there are many studies of flow in open cavities and the resulting effects on heat transfer [11, 13]. However, no study has examined the effects of cantilever beam applications on the thermal behaviour of residential buildings. However, a few studies related to the energy-saving designs for buildings' frontispieces are available in the literature. One of the most comprehensive studies on this subject was conducted by Prianto and Depecker [17]. In their study, the effects of projecting balconies on indoor air quality were investigated computationally in detail. Lai and Wang [18] examined the key factors in building frontispiece design which saves energy in Taiwan by utilizing the simulation software eQUEST. Chan and Chow [19] investigated an ordinary residential flat with a balcony built into the living room and its energy performance utilizing the typical weather data set of Hong Kong, which has a subtropical climate. Chand et al. [20] experimentally investigated the influence of balconies on ventilation, which induces the prevailing wind forces. The experimental results showed that provision of balconies changes wind pressure distribution on the windward wall but does not display considerable alteration in it on the leeward side. Namli (21) studied airflow and heat transfer in built-in balcony applications, using a computational investigation based on the open-ended structure approach. The numerical results indicated that the built-in balcony application on buildings reduces heat loss for all Rayleigh numbers considered.

In this study, the main problem is the heat loss of the residential buildings due to the entrances on the external geometry of the buildings. The entrance of the residential buildings such as the cantilever beam applications was considered as a cavity. Then, the heat loss from the exterior surface of the residential building was determined by utilizing open-ended enclosure and extended boundaries approaches and calculating the Nu number. That is, the open-ended cavity approach is adapted to this heat loss problem related to the residential buildings. A similar study is not available in the literature. As mentioned above, current studies in the literature are usually concerned with examining the effects of exterior geometry on the interior ventilation of a building. Accordingly, the cantilever beam application has been considered as a form of the cavity and have been subjected to numerical investigation in terms of building thermal performance. Considered all these, the aim of this study is that the thermal behaviour of residential buildings with cantilever beams, which are often used for creating balconies or other extensions above ground level in residential architecture, was investigated computationally by means of the open-ended enclosure approach. For this purpose, a parametric study was conducted for various ratios of cantilever beam depth/cantilever beam height (d/H) and Rayleigh numbers using a computer program encoded in Fortran when there was no wind for laminar flow. In the computational analysis, according to Boussinesq's approach (for $\Delta T \leq 20$ °C), the change in density caused by heat difference was taken into account only when calculating buoyancies. The other density values in the analysed equations are assumed to be constant in this temperature range. However, the air taken into account in the analysis was accepted as the Newtonian fluid, and Pr=0.71 was accepted. Vorticity, stream function and energy equations were analysed together within the boundary conditions defined. The findings obtained were arranged in the counter diagrams for both streamlines and isotherms. To determine the heat loss, the mean Nusselt numbers were defined for the outer vertical wall of L within the enclosure for each case.

Analyses were conducted for Rayleigh numbers ranging from 10^3 to 10^6 so long as they stayed in the laminar flow. In the calculations, values of 0.0, 0.2, 0.4, 0.6, 0.8 and 1.0 were used as the ratios of d/H. In this way, the analysis for the various ratio values of d/H for especially high Rayleigh numbers was obtained in the range of $0.0 \leq d/H \leq 1.0$. As a result of the discussion of the findings obtained, the effects of the various ratios of d/H and the Rayleigh numbers on the mean Nusselt number calculated along the L surface (the outer vertical wall of the enclosure) were examined.

FORMULATION AND NUMERICAL SCHEME

The two-dimensional enclosure analysed in this work, which has an open side (open-ended cavity) of height ($H+L$) and width B, is shown simply as a schematic diagram in Fig. 1. The vertical and horizontal walls of the building are heated to a constant temperature t_H, while the horizontal ground of the solution section is maintained at a constant temperature t_C, which is lower than t_H The surrounding fluid which interacts with the open-ended enclosure is at an ambient temperature t_∞, which is in thermal equilibrium with t_C. The working fluid atmospheric air and Newtonian, and the flow is presumed to be incompressible and laminar. The fluid properties are constant except for the density ρ, which is assumed to differ linearly from the temperature in reference to Boussinesq's approximation. Joule heating and viscous dissipation and were neglected in this study. The working fluid was treated as air whose Prandtl number was equal to 0.71.

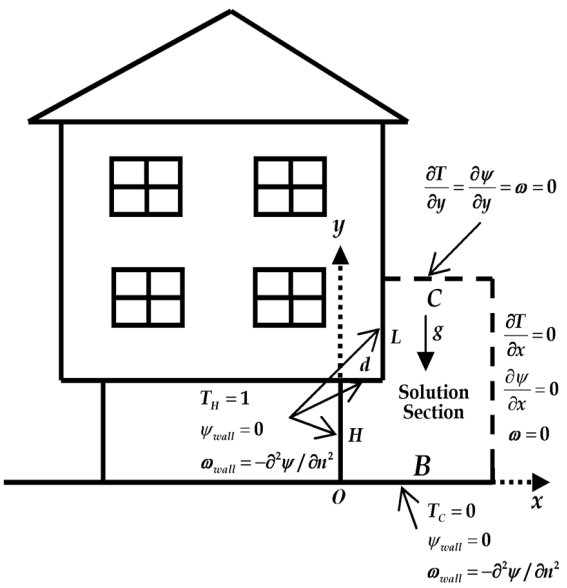

Figure 1. Schematic representation of solution domain

Considering the aforementioned assumptions, the governing equations can be expressed in the dimensionless form of stream function-vorticity equations as follows:

$$\frac{\partial}{\partial x}\left(T\frac{\partial \psi}{\partial y}\right)-\frac{\partial}{\partial y}\left(T\frac{\partial \psi}{\partial x}\right)-\frac{\partial}{\partial x}\left(\frac{1}{\mathrm{Pr}}\frac{\partial T}{\partial x}\right)-\frac{\partial}{\partial y}\left(\frac{1}{\mathrm{Pr}}\frac{\partial T}{\partial y}\right)=0 \quad (1)$$

$$\frac{\partial}{\partial x}\left(\omega\frac{\partial \psi}{\partial y}\right)-\frac{\partial}{\partial y}\left(\omega\frac{\partial \psi}{\partial x}\right)-\frac{\partial}{\partial x}\left(\frac{\partial \omega}{\partial x}\right)-\frac{\partial}{\partial y}\left(\frac{\partial \omega}{\partial y}\right)=0 \quad (2)$$

$$\frac{\partial^2\psi}{\partial x^2}+\frac{\partial^2\psi}{\partial y^2}=-\omega \quad (3)$$

where

$$\omega=\frac{\partial v}{\partial x}-\frac{\partial u}{\partial y}\ ,\ u=\frac{\partial \psi}{\partial y}\ ,\ v=-\frac{\partial \psi}{\partial x} \quad (4)$$

Equations (1)-(3) are the equations of the dimensionless temperature, vorticity and stream function, respectively.

The Dimensionless Boundary Conditions

As is the case with Fig. 1, the dimensionless boundary conditions in the extended computational zone can be written as:

1. For the left vertical and horizontal walls of the enclosure at $x=0$ and $0\le y\le H$; $x=d$ and $H\le y\le L$;
at $y=H$ and $0\le x\le d$;

$$T_H=1\ ,\ \psi_{wall}=0\ ,\ \omega_{wall}=-\frac{\partial^2\psi}{\partial n^2} \quad (5)$$

2. For the bottom horizontal wall of the enclosure
at $y=0$ and $0<x\le B$;

$$T_C=\psi_{wall}=0\ ,\ \omega_{wall}=-\frac{\partial^2\psi}{\partial n^2} \quad (6)$$

3. For the $x-$ far field open boundary
at $x=B$ and $0<y\le H+L$;

$$\frac{\partial T}{\partial x}=\frac{\partial \psi}{\partial x}=\omega=0 \quad (7)$$

4. For the $y-$ far field open boundary
at $y=H+L$ and $d<x\le C$;

$$\frac{\partial T}{\partial y}=\frac{\partial \psi}{\partial y}=\omega=0 \quad (8)$$

where ω_{wall} is the vorticity value at the wall and is the outer normal of the surface. The vorticity at sharp corners requires special consideration. The vorticity bifurcation at the corners is basically taken into account via the introduction of two different vorticity values. The vorticity values of the sharp corner were calculated as the arithmetical average of the values of the two adjacent wall nodes. These circumstances were applied to calculate the relevant values for all solution section limitations when the steady-state numerical calculations were carried out. The temperature conditions at the sharp corners also require special attention. The discontinuity of the temperature at the rectangular intersection and base walls (the origin of the coordinate system

selected) was determined by taking into consideration the arithmetical average temperature of both walls at the corner and maintaining the connected nodes with the relevant temperatures of the wall.

Nusselt Numbers

The energy transported across the vertical inner wall of the residential building is expressed as local and mean Nusselt numbers. Accordingly, for the outer vertical wall (surface L) of the residential building, the local Nusselt numbers can be derived from the dimensionless temperature gradients in the normal direction of the surface as shown in the following relationship:

$$Nu_{y,L} = \left.\frac{\partial T}{\partial n}\right|_{x=d} \tag{9}$$

and then the mean Nusselt number along the outer vertical wall (L) is;

$$Nu = \frac{1}{L}\int_{H}^{L} \left.\frac{\partial T}{\partial n}\right|_{x=d} dy. \tag{10}$$

where n denotes the normal direction of the surface. The integration of Eq. (10) was carried out by applying the trapezoidal rule. This equation of the mean Nusselt number is used to stand for all the heat transfer findings in this study.

Numerical Methods

The equations for energy transport, vorticity transport and the stream function together with the boundary conditions represent the problem under consideration. In this study, the equations for vorticity transport and energy transport were calculated using the alternating direction implicit (ADI) method, which is a finite difference technique [22]. After that, the equation of the stream function was calculated using the Gaussian successive over-relaxation (SOR) technique [23]. Convective terms were predicted using the upwind differencing scheme. For diffusive terms, the central difference scheme was used. In the present study, a uniform grid distribution was applied. Many calculation experiments were carried out to achieve grid-independent results for all the field variables. During testing and evaluation of the grid-independence of the present prediction scheme, many numerical calculations were performed for higher Rayleigh numbers. During the testing and evaluation of grid independence of the current prediction, several numerical calculations were conducted for higher Rayleigh numbers. These assesments found out that a uniformly spaced grid of 161x101 for a C-shape cavity can be used to correctly define the fluid flow and heat transfer processes within the open-ended enclosure, especially close to the walls while keeping up with rapid changes of the dependent variable. Further increments in the grid point numbers acquired the same results. When the following convergence criteria were ensured for each point in the solution zone, the analyses were accepted to converge:

$$\left|\frac{\varphi_{new} - \varphi_{old}}{\varphi_{new}}\right| \le 10^{-4} \tag{11}$$

where ϕ stands for the dimensionless values of stream function ψ, vorticity ω and temperature T.

Model Validation

Verification of the used model is considered a significant part of this study. To examine the validity of the numerical results, the present numerical model with corresponding wall boundary conditions was verified through comparison with an experimental study conducted by Abu-Mulaweh et al. [24] as shown in Fig. 2. For the laminar boundary layer airflow of buoyancy-induced natural convection along a two-dimensional vertical forward step, some considerations were presented in that work. The upstream and downstream walls and step itself were maintained at a uniform and constant temperature. Fig. 2 illustrates the effect of step height on the local Nusselt number's axial variation downstream of the step (surface L) for the case of Δ T=23°C (between the free stream and the heated wall), Ra=6.134×10^7 and step height of 16 mm. It is seen in this comparison that the results of this study match on a large scale with the results of Abu-Mulaweh et al. [24]. The results of the present study were also verified by comparison with the numerical results of Asan and Namli [25, 26].

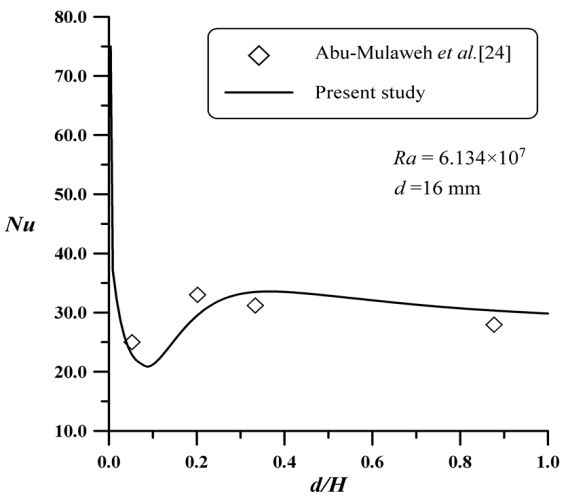

Figure 2. Local Nusselt number vs. y on the outer vertical wall (surface L).

For the values of the velocities and temperatures, the conditions of the open boundary were approximated by denoting the normal gradients at zero at these locations. The

aforementioned recommendations ensured sufficient precision on the condition that the solution zone was enlarged far enough. Penot [27] numerically carried out a natural convection study in a two-dimensional open-ended enclosure in which all vertical and horizontal walls were isothermal. The author also calculated the governing equations in an extended computational zone by taking account of the boundary conditions of the far field. In addition, according to Vafai and Ettefagh [11], the properties of fluid flow and heat transfer in an enclosure which is open on one side and in its immediate surroundings will not vary considerably assured that the solution zone is enlarged at last 60 times the cavity height in cases of high Rayleigh numbers. On the contrary, LeQuere et al. [28] applied a maximum extension of only about twice the enclosure height in determining the outer boundary conditions in order to calculate the laminar natural convection in a heated open-ended cavity. In the present study, the extension of the solution zone was four times the cantilever beam height of the residential building (H), and the ratios of d/H were varied from 0.05 to 1.0.

RESULTS AND DISCUSSION

In the present study, various prevalent parameters such as Rayleigh number and the ratio of d/H were analysed. Most of the results were attained for cases in which the building walls had a dimensionless temperature of $T_H = 1$ and the ground had a dimensionless temperature of $T_C = 0$ .The working fluid was air, which has a Prandtl number of 0.71. The calculations were carried out for cantilever beam d/H ratios of 0, 0.2, 0.4, 0.6, 0.8, 1.0. Rayleigh numbers ranged from Ra = 10^3 to Ra = 10^6 so long as they stayed in the laminar flow.

In this study, in order to remove the influences of the far field analysis on the properties of the flow field and heat transfer in an enclosure which was open on one side and in its adjacent area, the open boundaries were properly enlarged four times the height of the enclosure in both directions. Only the portion focused on the open-ended zone and its adjacent area was introduced in the form of contour line graphics (in terms of isotherms and streamlines) to demonstrate the fields of the fluid flow and temperature results in the enclosure. The isotherm values began with 0.0 and increased by 0.05 for all contour line graphics of the dimensionless temperature in this study. For all solid boundaries, the streamline contour values were taken as zero and increased by 0.5 for Ra = 10^3, 1.0 for Ra = 10^4, 2.0 for Ra = 10^5, and 5.0 for Ra = 10^6. First, the effects of different d/H ratios, taking account the Rayleigh number, on the flow and temperature field were discussed with the help of comparing streamlines and isotherms as shown in Fig. 3. At the same time, with the graphics given in Fig. 4 and Fig. 5, in both situations and with different Rayleigh numbers, the change in the mean Nusselt numbers calculated along the outer vertical wall (surface L) was examined with respect to the d/H ratio.

The effect of Rayleigh number on the streamlines and the isotherms for different flow cases was illustrated in Fig. 3. As Fig. 3a shows, for Ra = 10^3, the heat transfer in the enclosure and on the vertical and horizontal walls of the residential building takes place predominantly by way of the conduction mechanism. Nevertheless, heat transfer via the convection mechanism is definitely not negligible, as shown in Fig. 3a by the isotherm distortion on the open side. When the hot buoyant fluid escapes from the restraint at the top of the horizontal surface, it climbs like a buoyant plume into the outdoor space. Due to this ejection mechanism [11, 12], the cold fluid from the outdoor space crawls into the open enclosure, and meanwhile, the hot fluid departs in the same way. The intensity of the ejection mechanism at low Ra numbers (Ra = 10^3 and Ra = 10^4) gradually decreases as the d/H ratio increases, whereas this intensity at higher Ra numbers (Ra=10^5) generally increases as the d/H ratio increases. For Ra = 10^6, the intensity of the ejection mechanism remains unstable, and this intensity has the highest value at a d/H ratio of 0.4. Moreover, the ejection mechanism also gives rise to energy transfer from the building walls of the enclosure to the neighbouring fluid. In addition, the fluid flow area in an enclosure which is open on one side is not symmetric around the middle-height plane for low Ra numbers. The reason is that the ejection mechanism, which acts on the hot input fluid, achieves a higher velocity in connection with the dropout flow when compared to the incoming flow. Therefore, the incoming cold fluid replaces a larger part of the gap plane than the hot exiting flow as a direct consequence of mass conservation. Furthermore, it can be seen in Fig. 3c and Fig. 3d that a single clockwise vortex is observed in the enclosure except for higher Rayleigh numbers (Ra =10^5 and Ra= 10^6) and the eye of the vortex is located at the top of the cross-section. With an increase in the Rayleigh number, a multi-eyed clockwise vortex appears in the enclosure. When the Rayleigh number increases, the clockwise vortex speed in the open-ended enclosure increases as well.

Accordingly, with an increase in Rayleigh number (Ra=10^5 and Ra=10^6), while the buoyancy force intensity increases, the thermal boundary layer thickness along the L surface decreases. Moreover, the flow penetrates into the cavity especially for higher Rayleigh numbers, filling the entire cavity with an increasing d/H ratio. As the Rayleigh number increases further, the cold fluid penetrates the cavity at much higher velocity. Then, as the temperature gradient increases because of the decrease in the thermal boundary layer thickness, the heat transfer from the L surface (the outer vertical wall within the enclosure) to the fluid increases. This increase in the heat transfer can be seen clearly in Fig. 4 and Fig. 5.

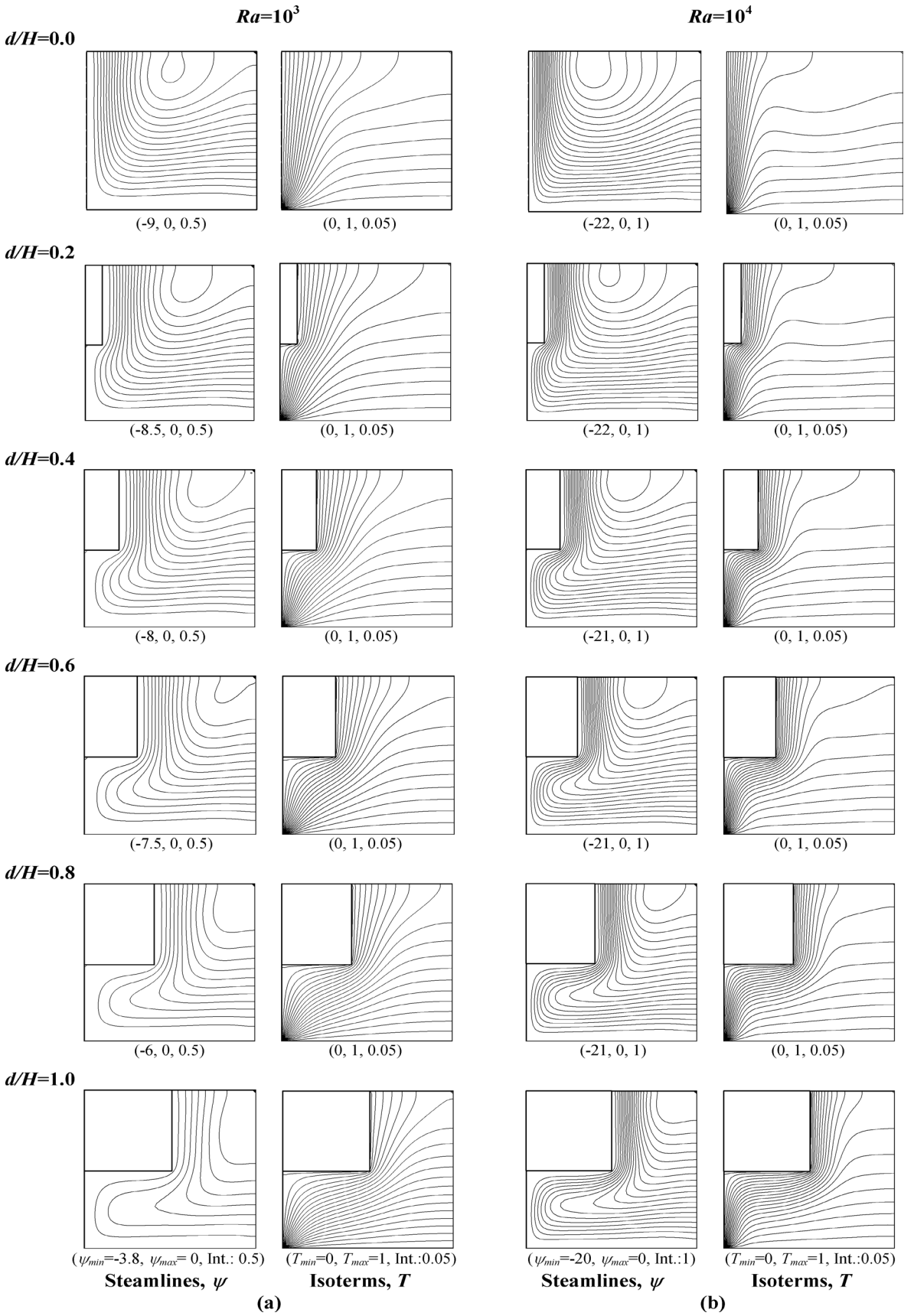
Ra=10^3
Ra=10^4
d/H=0.0
(-9, 0, 0.5)
(0, 1, 0.05)
(-22, 0, 1)
(0, 1, 0.05)
d/H=0.2
(-8.5, 0, 0.5)
(0, 1, 0.05)
(-22, 0, 1)
(0, 1, 0.05)
d/H=0.4
(-8, 0, 0.5)
(0, 1, 0.05)
(-21, 0, 1)
(0, 1, 0.05)
d/H=0.6
(-7.5, 0, 0.5)
(0, 1, 0.05)
(-21, 0, 1)
(0, 1, 0.05)
d/H=0.8
(-6, 0, 0.5)
(0, 1, 0.05)
(-21, 0, 1)
(0, 1, 0.05)
d/H=1.0
(ψmin=-3.8, ψmax= 0, Int.: 0.5)
(Tmin=0, Tmax=1, Int.:0.05)
(ψmin=-20, ψmax=0, Int.:1)
(Tmin=0, Tmax=1, Int.:0.05)
Steamlines, ψ
Isoterms, T
(a)
Steamlines, ψ
Isoterms, T
(b)

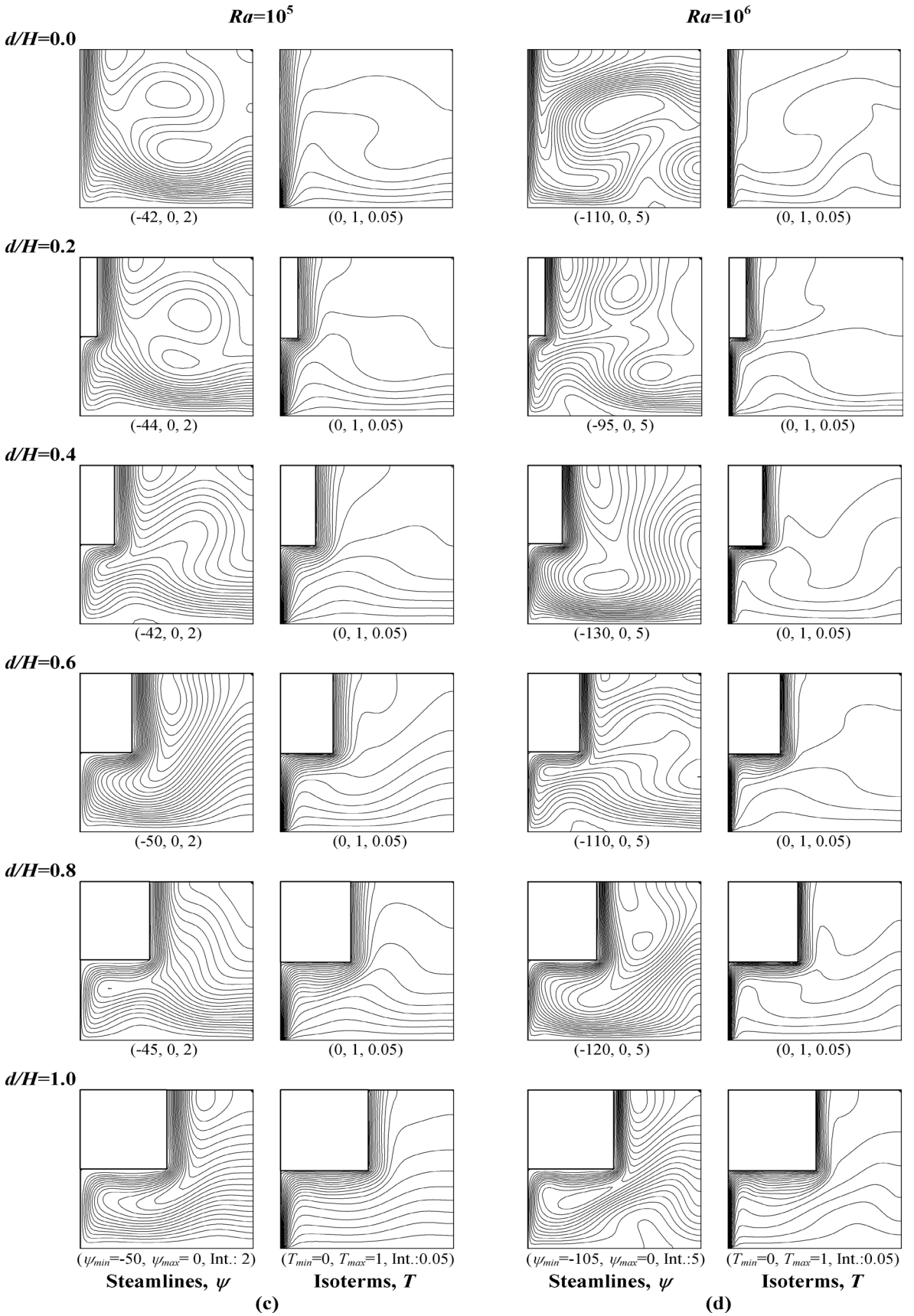

Figure 3. The effect of the ratio of cantilever beam depth/cantilever beam height (d/H) and Rayleigh number upon streamlines and isotherms: (a) $Ra=10^3$, (b) $Ra=10^4$, (c) $Ra=10^5$, (d) $Ra=10^6$

As shown in Fig. 3a and Fig. 3b, for lower Rayleigh numbers ($Ra=10^3$ and $Ra=10^4$), one can observe a tendency for the speed of the clockwise vortex to decrease because of the intensity of the buoyancy force with an increase in the d/H ratio. As a result, the thickness of thermal boundary layer increases along the L surface in this situation. As this happens, the temperature gradient decreases and the heat transfer, which occurs along the L surface from the hot surface to the fluid, shows a tendency to decrease. On the contrary, as shown in Fig. 3c and Fig 3d, for higher Rayleigh numbers ($Ra=10^5$ and $Ra=10^6$), a multi-eyed clockwise vortex appears in the enclosure, causing the speed of the clockwise vortex to increase for some d/H ratios while it decreases for other d/H ratios. For example, for $Ra=10^5$ and d/H=0.4 the speed of the clockwise vortex decreases in comparison with the no-cantilever-beam-application case (d/H=0.0). In the same way, for $Ra=10^6$ and d/H=0.2 the speed of the clockwise vortex decreases in comparison with the no-cantilever-beam-application case. These decreases in the speed of the clockwise vortex for higher Rayleigh numbers can be explained by the fact that there are reversed flows in the ground (surface B). In the case that there is no reversed flow in the ground, the fluid that starts to move because of the effects of the buoyancy force intensity together with the increase in the d/H ratio can move more easily in the cavity. With this freedom of movement, it can be understood that the ejection mechanism is more effective in these situations. Afterward, the cold air from the surrounding area quickly infiltrates into the lower part of the open cavity to take up the separating fluid. This suction mechanism creates an almost parallel flow over the entire vertical wall in the open-ended cavity. Although there is an irregular flow pattern in the enclosure at higher Rayleigh numbers, the thickness of the thermal boundary layer along the L surface increases with the increasing d/H ratio. As the temperature gradient decreases due to the increasing thickness or thermal boundary layer, the heat transfer from the L surface to the fluid decreases gradually. This decrease in the heat transfer can be seen clearly in Fig. 4 and Fig. 5. In these figures, the distribution of the mean Nu number is given only for L except for d+H+L because d consistently varies with the d/H ratio. Furthermore, in comparison with H in residential buildings, L actually has a much bigger value. As can be seen in Fig. 4, as the d/H ratio increases, the mean Nu number along the L surface does not change significantly at low Ra numbers ($Ra = 10^3$ and $Ra = 10^4$), but the mean Nu number along the L surface at higher Ra numbers ($Ra=10^5$ and $Ra=10^6$) decreases considerably as the d/H ratio increases. It can also be seen from Fig. 4 that the Nu number is not stable for high Ra numbers (especially for $Ra = 10^6$). As can be seen in Fig. 5, there is no significant change in the mean Nu number when the d/H ratio increases, whereas a significant decrease in the mean Nu number as the d/H ratio increases can be observed for values above $Ra=10^4$. Consequently, as can be seen in Fig. 4 and Fig. 5, the decreases in heat transfer along the L surface (the outer vertical wall of the enclosure) with the increasing d/H ratio for the values of $Ra=10^3$, 10^4, 10^5 and 10^6 are approximately 28%, 11%, 31% and 30% in comparison with the no-cantilever-beam-application case, respectively.

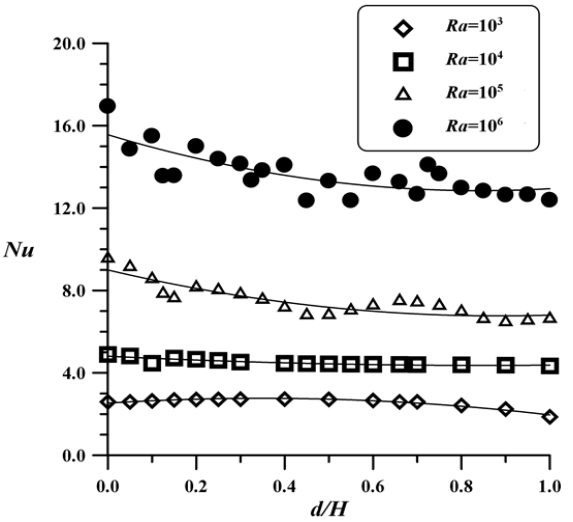

Figure 4. The effect of the ratio of cantilever beam depth/cantilever beam height (d/H) upon the mean Nusselt number along the L surface

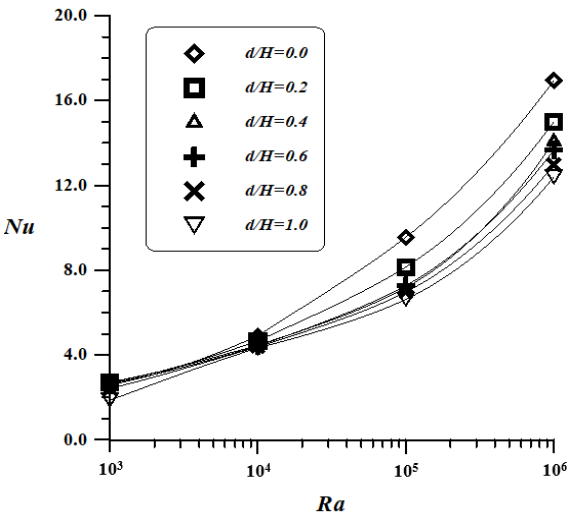

Figure 5. The effect of Rayleigh number upon the mean Nusselt number along the L surface

CONCLUSION

In this study, the thermal behaviour of buildings with cantilever beams under winter day boundary conditions was investigated numerically by means of the open-ended structure approach. For this purpose, a parametric study was performed for various ratios of cantilever beam d/H and Rayleigh numbers using a computer program when there was no wind for laminar flow. Analyses were con-

ducted for Rayleigh numbers varying from 10^3 to 10^6. The analyses were carried out for d/H ratios of 0.0, 0.2, 0.4, 0.6, 0.8 and 1.0. The working fluid was air (Pr=0.71).

The most important effect of the heat loss within the residential building cantilever beam (within the cavity) is the ejection mechanism. The intensity of the ejection mechanism at low Ra numbers (Ra = 10^3 and Ra = 10^4) gradually decreases as the d/H ratio increases, whereas this intensity at higher Ra numbers (Ra=10^5) generally increases as the d/H ratio increases. For Ra = 10^6, the intensity of the ejection mechanism remains unstable, and this intensity has the highest value at a d/H ratio of 0.4. Moreover, the ejection mechanism also gives rise to energy transfer from the building walls of the enclosure to the neighbouring fluid.

The ejection mechanism also affects the thickness of the thermal boundary layer in the cavity. The thickness of the thermal boundary layer decreases with the increasing intensity of the ejection mechanism. Eventually, as the temperature gradient increases because of the decrease in the thermal boundary layer thickness, the heat transfer from the L surface (the outer vertical wall within the cavity) to the surrounding fluid increases. According to all these, in general, the mean Nu number, which is an indication of heat loss from the cavity, along with the outer vertical wall (surface L) of the residential building decreases with an increase in the d/H ratio for all Rayleigh numbers. This decrease in the mean Nu number is evident for Ra≤10^4, but after Ra=10^5 it appears to be more pronounced. To have minimum heat loss from residential buildings under winter day boundary conditions, it is suggested that the ratio of d/H be between 0.2 and 0.5.

NOMENCLATURE

H cantilever beam height of building (m)
d cantilever beam depth of building (m)
L outer vertical wall of the enclosure (m)
d/H the ratio of cantilever beam depth/cantilever beam height
Pr Prandtl number
Ra Rayleigh number
t_∞ ambient temperature (°C)
t_H hot wall temperature of the enclosure (K)
t_C cold wall temperature of the enclosure (K)
Δt temperature difference
T dimensionless temperature
Nu_y local Nusselt number
Nu the mean Nusselt number
g acceleration of gravity (m/s2)
k the coefficient of thermal conductivity (W/mK)
h the coefficient of convective heat transfer (W/m2K)
n the normal direction of the surface
Int. Interval

Greek symbols

ψ dimensionless stream function
ω dimensionless vorticity
ν kinematic viscosity (m2/s)
β the coefficient of volume expansion (1/K)
α thermal diffusivity (m2/s)

Subscript

H hot wall
C cold wall
min minimum
max maximum

References

1. Raithby GD, Hollands KGT. Natural convection, in: Rohsenow WM, Harnett JP, Ganic EN, (Eds.), Handbook of Heat Transfer Fundamentals. second ed. McGraw–Hill, New York, 1985 (Chapter 6).
2. Ostrach O. Natural convection in enclosure, Journal of Heat Transfer 110 (1988) 1175–1190.
3. Tavares MCP, Goncalves HJP, Bastos JNTFC. The glazing area in residential buildings in temperate climate: The thermal–energetic performance of housing units in Lisbon. Energy and Buildings 140 (2017) 280-294.
4. Aimee Byrne A, Byrne G, O'Donnell G, Robinson A. Case studies of cavity and external wall insulation retrofitted under the Irish home energy saving scheme: Technical analysis and occupant perspectives. Energy and Buildings 130 (2016) 420-433.
5. Magalhaes SMC, Leal VMS, Horta IM. Modelling the relationship between heating energy use and indoor temperatures in residential buildings through artificial neural networks considering occupant behavior. Energy and Buildings 151 (2017) 332-343.
6. Yousefi F, Gholipour Y, Yan W. A study of the impact of occupant behaviors on energy performance of building envelopes using occupants' data. Energy and Buildings 148 (2017) 182–198.
7. Jin X, Medina MA, Zhang X. On the placement of a phase change material thermal shield within the cavity of buildings walls for heat transfer rate reduction. Energy 73 (2014) 780–786.
8. Sorgato MJ, Melo AP, Lamberts R. The effect of window opening ventilation control on residential building energy consumption. Energy and Buildings 133 (2016) 1-13.
9. Selamet EE, Arpaci VS, Borgnakke C. Simulation of laminar buoyancy–driven flows in an enclosure. Numerical Heat Transfer, Part A 22 (1992) 401–420.
10. Chan YL, Tien CL. A numerical study of two–dimensional natural convection in square open cavities. Numerical Heat

Transfer 8 (1985) 65–80.
11. Vafai K, Ettefagh J. The effect of sharp corners on buoyancy–driven flows with particular emphasis on outer boundaries. International Journal of Heat and Mass Transfer 33 (1990) 2311–2328.
12. Vafai K, Ettefagh J. Thermal and fluid flow instabilities in buoyancy–driven flows in open–ended cavities. International Journal of Heat and Mass Transfer 33 (1990) 2329–2344.
13. Khanafer K, Vafai K, Lightston M. Mixed convection heat transfer in two–dimensional open–ended enclosures. International Journal of Heat and Mass Transfer 45 (2002) 5171–5190.
14. Elsayed MM, Chakroun W. Effects of aperture geometry on heat transfer in tilted partially open cavities. Journal of Heat Transfer 121 (1990) 819–827.
15. Khanafer K, Vafai K. Buoyancy–driven flows and heat transfer in open–ended enclosures: Elimination of the extended boundaries. International Journal of Heat and Mass Transfer 43 (2000) 4087–4100.
16. Khanafer K, Vafai K. Effective boundary conditions for buoyancy–driven flows and heat transfer in fully open–ended two–dimensional enclosures. International Journal of Heat and Mass Transfer 45 (2002) 2527–2538.
17. Prianto E, Depecker P. Characteristic of airflow as the effect of balcony, opening design and internal division on indoor velocity: A case study of traditional dwelling in urban living quarter in tropical humid region, Energy and Building 34 (2002) 401–409.
18. Lai CM, Wang YH. Energy–saving potential of buildings envelope designs in residential houses in Taiwan. Energies 4 (2011) 2061–2076.
19. Chan ALS, Chow TT. Investigation on energy performance and energy payback period of application of balcony for residential apartment in Hong Kong. Energy and Building 42 (2010) 2400–2405.
20. Chand I, Bhargava PK, Krishak NLV. Effect of balconies on ventilation inducing aeromotive force on low–rise buildings. Building and Environment. 33 (1998) 385–396.
21. Namli L., Effects of built–in balcony on thermal performance in residential buildings: A case study. Journal of Building Physics 40(2) (2016) 125–143.
22. Roache PJ. Computational Fluid Dynamics. Hermosa, Albuquerque, NM, 1982.
23. Young D. Iterative methods for solving partial differential equations of elliptical type. Transactions of the AMS – American Mathematical Society 76 (1954) 92.A
24. Abu–Mulaweh HI, Armaly BF, Chen TS. Laminar natural convection flow over a vertical forward–facing step. Journal of Thermophysics and Heat Transfer 10 (1996) 517–523.
25. Asan H, Namli L. Laminar natural convection in a pitched roof of triangular cross–section: summer day boundary conditions. Energy and Building 33 (2000) 69–73.
26. Asan H, Namli L. Numerical simulation of buoyant flow in a roof of triangular cross–section under winter day boundary conditions, Energy and Building 33 (2001) 753–757.
27. Penot F. Numerical calculation of two–dimensional natural convection in isothermal open cavities. Numerical Heat Transfer 5 (1982) 421–437.
28. LeQuere O, Humphery JAC, Sherman FS. Numerical calculation of thermally driven two–dimensional unsteady laminar flow in cavities of rectangular cross–section. Numerical Heat Transfer 4 (1981) 249–283.